Journal of Non-Newtonian Fluid Mechanics 266 (2019) 160–170

Contents lists available at ScienceDirect

Journal of Non-Newtonian Fluid Mechanics

journal homepage: www.elsevier.com/locate/jnnfm

Dripping-onto-substrate capillary breakup extensional rheometry of low-viscosity printing inks

Maxime Rosello[a], Samrat Sur[a], Bruno Barbet[b], Jonathan P. Rothstein[a,*]

[a] Department of Mechanical and Industrial Engineering, University of Massachusetts, Amherst, 01003
[b] Markem-Imaje Corp., 26501 Bourg Les Valence, France

ARTICLE INFO

Keywords:
Extensional rheology
Capillary breakup
Ink-jet fluids
Viscoelasticity
Filament thinning

ABSTRACT

In this manuscript, the capillary thinning dynamics of a series of solutions containing polymers commonly used in the coating industry as low-viscosity printing inks were studied. Four different polymer binders were studied in methyl-ethyl ketone. These included one acrylic polymer, one cellulose polymer and two vinyl polymers of different molecular weights. The dripping-onto-substrate capillary breakup extensional rheometry (CaBER-DoS) method was used to characterize the extensional rheology for solutions with viscosities as low as 3.5mPa.s. This technique is based on the measurement of the decay of a fluid filament under the influence of surface tension and has been shown to be capable of measuring relaxation times as low as 20 μs for weakly elastic liquids. The influence of the polymer concentration on the dynamics of filament breakup was investigated for each polymer solution and the results were compared to those obtained with different polymer binders. With an increase in polymer concentration, a critical polymer concentration was identified for the transition between the inertio-capillary, the visco-capillary and the elasto-capillary breakup regimes. With the onset of elasto-capillary breakup at moderate to high polymer concentrations, a delay in the filament breakup was observed due to an increase of the viscous and elastic stresses. This viscoelastic breakup delay would be detrimental to most ink jet printing applications. Within the elasto-capillary breakup regime, the transient extensional viscosity resulted in Trouton ratios ranging from just above the Newtonian limit of $Tr = 3$ to values close to $Tr = 100$.

1. Introduction

In many industrial processes, a wide range of printing and patterning technologies are currently being used to deposit well-defined 2D and 3D patterns of polymeric fluids onto both static and moving substrates. Innovations in printing technologies like inkjet printing have opened up a wide range of application spaces beyond their classical use in printing documents, photos and magazines. More recently these printing techniques have been extended to manufacture solar panel, electronics, optical devices and functional biomaterials [1–3]. Inkjet printing technologies can be separated into two classes: drop-on-demand (DOD) and continuous injket (CIJ) [2,3]. In the first, individual drops are created from pressure or displacement pulses from within the nozzle. In the second, a continuous jet is produced and allowed to break up into drops. In this way, a continous stream of drops is produced with the excess unneeded drops deflected into a gutter through either electrostatics or aerodynamics.

In order to understand the dynamics of either of these inkjet processes, one requires a deep understanding of the capillary breakup phenomena and of the rheology of the inkjet fluids. This is because the composition of inkjet fluids can be quite complicated with the relatively large fractions of low molecular weight polymers, particles and dyes added to the final composition. The addition of a polymer binders to a solution is especially relavent to jetting as it can make the ink weakly elastic resulting in some dramatic changes to the drop impact and filament breakup dynamics. For instance, satellite droplets in drop-on-demand devices can be eliminated by adding polymer to the solution, but that comes with a significant breakup delay [4]. Consequently, architecture, concentration and molecular weight of a polymer into the solution must be chosen wisely. Unfortunately, the low viscosity, weak elasticity and extremely short relaxation times of most commercial ink jet fluds have made them extremely challenging to characterize rheologically. The influence of polymers concentration on drop formation and filament breakup has been widely studied both experimentally and numerically for more elastic monodisperse polymer solutions in the dilute regime up to the coil overlap concentration, c^* [4,5]. These studies found that such flows typically involve high extension rates which can result in a strong increase in the transient extensional viscosity of the

* Corresponding author at: University of Massachusetts, Amherst, 01003
E-mail address: rothstein@ecs.umass.edu (J.P. Rothstein).

https://doi.org/10.1016/j.jnnfm.2019.03.006
Received 21 August 2018; Received in revised form 1 March 2019; Accepted 12 March 2019
Available online 12 March 2019
0377-0257/

polymeric fluid. The observable consequence of which has been shown to be the formation of long fluid threads [6,7] and a significant increase in the time required for the filament to break up into drops [8]. In order to be able to predict the breakup dynamics of inkjet fluids as they are printed, we will use a recently developed extensional rheometry technique known as dripping-onto-substrate capillary breakup extensional rheometry (CaBER-DoS) [9,10].

Our knowledge of extensional properties of fluids widened significantly with the development of elongational filament stretching methods, reviewed by McKinley and Sridhar [11]. In such devices, a liquid bridge is formed and becomes a filament whose minimum diameter evolution is recorded. In filament stretching methods, a cylindrical liquid bridge is formed between two plates. These plates are then moved appart with an exponential velocity profile, resulting in a constant extensional strain rate and significant strain on the polymeric liquid bridge and eventually its breakup [12]. This method is convenient for polymer melts and moderate viscosity solutions ($\eta_0 > 1$ Pa.s) and has enabled the measurement of polymer relaxation times of several seconds.

In filaments thinning techniques [13], after having filled the gap between plates with the fluid to be tested, the upper plate is moved and then stopped at a desired separation distance. The liquid bridge that is formed is unstable, and a result, it begins to thin down and breaks up under the action of capillary forces. Bazilevsky's device [13] has been further improved by a number of other researchers including Anna and McKinley [14] and is now sold under the name CaBER (Capillary Breakup Extensional Rheometry) by Thermo scientific. This is a common technique for determining the extensional rheology of viscoelastic fluids with viscosities as low as $\eta_0 = 70$ mPa.s and relaxation times as small as $\lambda = 1$ ms [15]. In order to reach even smaller relaxation times for even lower viscosity fluids, an alternate high speed filament stretching method has been developed under the name Cambridge Trimaster (CTM) [16]. It is based on the synchronized separation of the two pistons in order to get a centred filament. Using the CTM, Vadillo et al. [15] measured relaxation times as short as $\lambda = 80$ μs by for a series of solution of monodisperse polystyrene dissolved in diethyl phthalate (DEP) with concentration of polystyrene ranging from dilute to concentrated with solution viscosity of $\eta_0 = 12$ mPa.s. One limitation of high-speed CaBER measurements and the CTM is the inertial effects resulting from the dynamics of the rapid step stretch imposed by the motor motion. At the high velocities required to measure the breakup dynamics of low viscosity fluids, like printer inks, the rapid step strain can lead to oscillations in the filament that make measurement of extensional rheology difficult. In order to avoid inertial effects, Campo-Deano et al. [17] used a slow retraction method (SRM) to investigate filament thinning mechanisms of fluids with shear viscosities similar to water, $1 < \eta_0 < 3$ mPa.s, and very short relaxation times, $\lambda > 200$ μs. This experimental technique involves slowly separating the pistons just beyond the critical separation distance for which a statically stable liquid bridge can exist. At this point, the filament becomes unstable and the thinning and breaking process is initiated. This SRM technique avoids inertial effects allowing the authors to extract relaxation times as short as $\lambda = 240$ μs for dilute aqueous solutions of polyethylene oxide (PEO) with a molecular weight of $M_w = 10^6$ g/mol and shear viscosities between $1 < \eta_0 < 3$ mPa.s [17]. More recently, Keshavarz et al. [18] took advantage of the Rayleigh capillary instability breakup process [19] to develop a new technique called Rayleigh Ohnesorge Jetting Extensional Rheometry (ROJER). This method involved the application of a perdiocical radius disturbance to a fluid jet in order to trigger a capillary instability and the tracking of the perturbation necks diameter until the jet breakup. Like all the techniques cited above, it allows the measurement of the fluid relaxation time as well as the Hencky strain, the strain rate and the transient extensional viscosity in the filament. Recently, Greiciunas et al. [20] were able to measure relaxation times with this technique down to $\lambda = 100$ μs for solutions with shear viscosities as low as $\eta_0 = 3$ mPa.s.

Amazingly, in order to characterize common inkjet printing inks, one often requires a device that can experimentally characterize the extensional rheology of polymeric solutions with relaxation times even lower than those described above. The time scales involved in the jetting process are on the order of microseconds, while the shear and extension rates experienced by the fluid can be on the order of a million reciprocal seconds [4]. As a result, viscoelastic polymeric solutions with relaxation times on the order of ten microseconds can have a significant impact on the jet formation and breakup. These relaxation times of inkjet fluids are often beyond the limit of the state of the art of extensional rheology characterization described above. For that reasons, in this paper, we will utilize the dripping-onto-substrate capillary breakup extensional rheometry method (CaBER-DoS) developed by Dinic et al. [9,10]. In this measurement technique, a single drop of fluid is dispensed at a relatively low flow rate onto a substrate which is placed at a fixed distance below the exit of the nozzle. Under the appropriate experimental conditions, a filament is formed when the droplet wets the substrate. By capturing the droplet on the substrate and not allowing it to fall, a capillary breakup extensional rheology measurement is initiated without the inertial effects associated with the moving of the top/bottom plate. Additionally, compared to the slow retraction method, CaBER-DoS is better suited for highly volatile fluid, like the methyl ethyl ketone (MEK) used here, because the experiments are performed much more quickly thereby limiting the effect of evaporation. Dinic et al. [10] succesfully measured extensional properties of a large variety of fluids, including a commercially-available printing ink, and were able to characterize fluids with relaxation times as low as $\lambda_E = 0.3$ ms. Sur et al. [21] extended their work to relaxation times an order of magnitude by measuring dilute PEO aqueous solutions with relaxation times as low as 20 μs [21].

In the present work, the extensional rheology of several solutions of polymers commonly used in the printing industry was studied so that the impact of polymers on the dynamics of jet formation and breakup into drops and its implications on the printability of inkjet fluids could be better understood in the context of real ink formulations. One of the differences between this study and other similar works reported in literature [9,10,21] is that, as is common in ink jet fluids, all the polymer solutions studied here were in the semi-dilute regime. This is the case even though the molecular weight of the polymers used here were all low, $M_w < 60{,}000$ g/mol, because the polymer concentration was increased well beyond the coil overlap concentration, c^*. The solutions studied here had shear viscosities as low as $\eta_0 \sim 3$ mPa.s and the polymers were all highly polydisperse. This chemical complexity, when added to the intense shearing upstream within the ink jet printer nozzle and the enormous extension rates experienced during the jet thinning and breakup makes predicting the dynamics of jet breakup and the impact of different additives on the viability of different inks extremely challenging. This is especially true when the fluid rheology cannot be fully characterized at the deformation rates at which these inks are processed. In the present work, we used CaBER-DoS to study the influence of the polymer concentration, polymer chemistry and polymer molecular weight on extensional viscosity, relaxation time and jet breakup. Of great interest were the transitions in filament thinning between inertia-dominated, viscous-dominated and elasticity-dominated regimes. These transitions were found to strongly correlate to the reduction in the size of satelite drops formed during jetting and a delay in the breakup of fluid jets into drops which could negatively impact the jetability of a given ink formulation.

2. Experimental setup

A schematic diagram of the dripping-onto-substrate capillary breakup extensional rheology (CaBER-DoS) experimental setup is presented on Fig. 1. In the CaBER-DoS experiment, a liquid drop was formed at the nozzle tip with a diameter of $D_{nozzle} = 800$ μm using a syringe pump (KD Scientific). The flow rate was maintained low enough to remain in the dripping regime and so that the motion before wetting

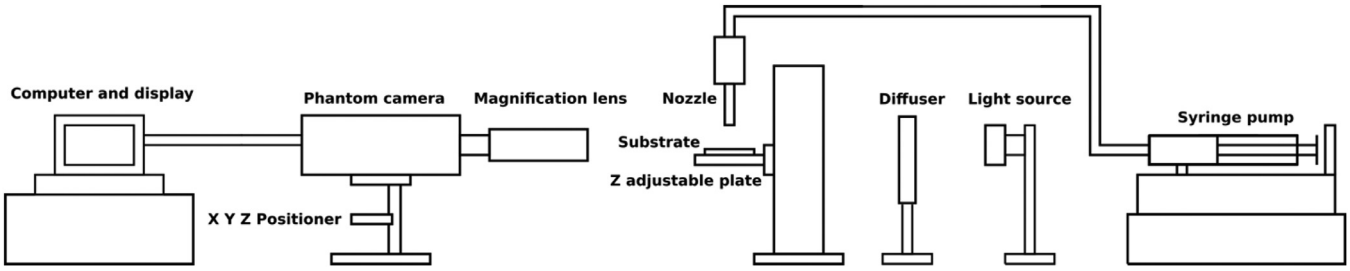

Fig. 1. Schematic diagram of the dripping-onto-substrate capillary breakup rheometry (CaBER-DoS) setup.

was only driven by gravity. The substrate was made of glass and was separated from the tip by a distance, $H_0 = 4$ mm. A high-speed camera (Phantom-Vision optics, V-4.2) was used to capture the filament breakup process at a frame rate of 20,000 fps using a window of 128×128 pixels. A 5 μm/pixel magnification was obtained using a long distance microscope lens (Edmund Optics). The diameter decay was digitized over time using an automated software called Edgehog (KU Leuven) which is capable of diameter measurements with sub-pixel resolution. The diameter data, however, are presented with a conservative estimate of the error of plus or minus one pixel or ±5 μm. A minimum of three independent experiments were performed for each ink jet fluid tested.

The thinning dynamics of a fluid filament in CaBER-DoS is driven by capillary forces which depends on the surface tension, σ, and the local curvature of the filament. The capillary thinning is resisted by a combination of fluid viscosity, inertia, and elasticity depending on the fluid physical and rheological properties and the size of the filament. The shape of the filament and the rate of draining can also be influenced by gravity although in most instances it can be neglected. The Bond number, $Bo = \rho g R^2/\sigma$, compares the influence of gravity to surface tension. Here, ρ is the density, g is the acceleration of gravity, R is the radius of the filament and σ is the surface tension. In all the experiments presented in this paper, a diameter of $D_0 = 250$ μm was chosen to be the initial diameter at $t = 0$ s. This choice is a bit arbitrary, but to achieve good results as the filament decayed, a very high magnification was required making it impossible to observe the diameter decay for larger filaments. All tested fluids had densities between $\rho = 800\,\mathrm{kg/m^3}$ and $900\,\mathrm{kg/m^3}$ and a surface tension of $\sigma = 24\,\mathrm{mN/m}$ which results in a maximum Bond number $Bo = 0.02$. At this Bond number, Clasen et al. [22] demonstrated that gravitational effects could be neglected in CaBER experiments for $Bo < 0.2$.

The competition between inertia, viscosity and elasticity in filament thinning processes give rise to three distinct filament breakup regimes known as the inertio-capillary, the visco-capillary and the elasto-capillary regime [23,24]. A number of important dimensionless groups characterize the necking process. These include: the Ohnesorge number, $Oh = \eta_0/(\rho\sigma R_0)^{1/2}$, which represents a balance of the inertial and viscous forces for a slender filament; the intrinsic Deborah number, $De_0 = \lambda_E/(\rho {R_0}^3/\sigma)^{1/2}$, which represents the ratio of the characteristic relaxation time of the fluid to the inertial timescale of the flow; and the elasto-capillary number, $Ec = \lambda_E\sigma/\eta_0 R_0$, which represents a ratio of the characteristic relaxation time of the fluid and the viscous timescale of the flow. In these dimensionless groups, η_0 is the shear viscosity of the fluid, R_0 is the radius of the filament, σ is the surface tension, ρ is the density and λ_E is the relaxation time in extension. For low-viscosity inelastic fluids, $Oh \ll 1$ and $De_0 \ll 1$, the thinning dynamics are driven by the competition between inertia and capillary forces and the filament radius follows a power law with an exponent of 2/3 [23],

$$\frac{R(t)}{R_0} = 0.8\left(\frac{\sigma}{\rho R_0^3}\right)^{1/3}(t_c - t)^{2/3} = 0.8\left(\frac{t_c - t}{t_R}\right)^{2/3}. \quad (1)$$

Here t_c is the filament breakup time and $t_R = (\rho {R_0}^3/\sigma)^{1/2}$ is the Rayleigh time which is a characteristic timescale for the breakup of fluids in this inertio-capillary regime [9,10]. The prefactor in Eq. (1) has been reported to be between 0.64 and 0.8 with some experimental measurements finding values as large as 1.0 [17,25–27].

For more viscous inelastic fluids with, $Oh >> 1$ and $Ec << 1$, the filament is known to decay linearly with time [28],

$$\frac{R(t)}{R_0} = 0.0709\left(\frac{\sigma}{\eta_0 R_0}\right)(t_c - t) = 0.0709\left(\frac{t_c - t}{t_v}\right). \quad (2)$$

Here, $t_v = \eta_0 R_0/\sigma$, is the characteristic viscous timescale for breakup. The transition between inertio-capillary and visco-capillary regimes has been shown by Clasen et al. [23] to occur at an Ohnesorge number of $Oh = 0.2077$.

For viscoelastic liquids such as the polymer solutions studied her, an elasto-capillary thinning regime can also exist. In this regime, the radius is known to decay exponentially with time for fluids well characterized by an Oldroyd-B or FENE-P model [14,29–31],

$$\frac{R(t)}{R_0} = \left(\frac{G R_0}{2\sigma}\right)^{1/3} \exp\left(-\frac{t}{3\lambda_E}\right). \quad (3)$$

Here G is the elastic modulus and λ_E is the relaxation time of the solution in an extensional flow. A transition from the inertio-capillary to the elasto-capillary regime has been shown for intrinsic Deborah numbers above $De_0 > 1$ while the transition from an visco-capillary to an elasto-capillary thinning has been shown to occur above an elasto-capillary number of $Ec > 4.7$ [23].

The use of analytical thinning regimes can be particularly helpful for the fast and accurate prediction of fluid behaviours in industrial processes. Unfortunately, in the literature, few examples deal with actual industrial fluids. This is why, in the present work, a special attention has been given to the influence of the polymer concentration onto the thinning regime.

2.1. Materials

The study focused on four different polymeric binders: Paraloïd™ B-66 (Dow) which is an acrylic polymer mainly used for surface coating compounds and printing inks; CAB-381-2 (Eastman) which is a cellulose acetate butyrate polymer; and Vinnol E15/45 M and Vinnol E22/48A (Wacker Chemie), which are vinyl chloride ter-polymer and co-polymers respectively. The molecular weights and coil overlap concentrations of each of these polymers listed in Table 1 were either provided by the suppliers directly or measured by our collaborators at Markem-Imaje. The solvent for each solution was methyl ethyl ketone (MEK), which has a zero-shear viscosity of $\eta_s = 0.43$ mPa.s and an equilibrium surface tension with air of $\sigma = 24\,\mathrm{mN/m}$ at 20°C [32]. The time scales involved in the CaBER-DoS breakup process are on the order of a few milliseconds or even less. Unfortunately, we did not have access to a measurement device capable of measuring the dynamic surface tension of our solutions at such a short surface lifetime. However, it is a reasonable assumption to make that the surface tensions of the fluid filaments formed

Table 1
List of the polymers used in the experiments along with their chemical natures, molecular weights and coil overlap concentrations.

Name	Chemical Nature	M_n [g/mol]	M_w [g/mol]	PDI	c^* [wt%]
Paraloïd B66™	Acrylic	27,300	51,800	1.9	6.8
CAB-381-2	Cellulose	52,900	158,900	3.0	1.4
Vinnol E15/45M	Vinyl Chloride	28,900	67,700	2.3	3.7
Vinnol E22/48A	Vinyl Chloride	37,800	118,300	3.1	3.2

Table 2
Shear viscosity and reduced concentrations for the solutions tested.

Paraloïd B66				
c [wt%]	15%	20%	25%	30%
η_0 [mPa.s]	5	6.9	13.3	25
c/c^*	2.2	2.9	3.7	4.4
CAB-381-2				
c [wt%]	4%	5%	6%	
η_0 [mPa.s]	6.9	9.4	16.9	
c/c^*	2.9	3.7	4.4	
Vinnol E 15/45 M				
c [wt%]	8%	12%	16%	
η_0 [mPa.s]	3.5	7.9	17.5	
c/c^*	2.1	3.2	4.3	
Vinnol E 22/48 A				
c [wt%]	6%	8%	10%	
η_0 [mPa.s]	6	8.1	13	
c/c^*	1.9	2.5	3.1	

is equal to that of the solvent. This is because the rate of interface creation during filament breakup far outpaces the rate of diffusion of the dissolved polymer to the interface [33,34]. The density of each solution was measured and found be the same as the solvent to within measurement uncertainty, $\rho = 865\ \mathrm{kg/m^3}$.

As shown in Table 2, the reduced polymer concentrations of all the solutions tested were just above the overlap concentration, $c/c^* > 1$, in the semi-dilute regime. In the semi-dilute regime, polymer chains entanglements can lead to significant modifications of the fluid rheology. These entanglements enhance confinement and resistance to polymer motion leading to a fast increase in the solution's shear viscosity and the relaxation time with increasing molecular weight and concentration [35]. In extensional flows, like the CaBER experiments studied here, polymer entanglements can lead to a reduction in the extensibility of the polymer chain and a decrease in the strain hardening of the extensional viscosity compared to a dilute, unentangled solutions [36,37]. The polydispersity index in each case was found to be significantly greater than one, $PDI = M_w/M_n > 1$, meaning that polymers were not monodisperse, but were polydisperse. Polydispersity of the polymer can lead to issues, especially in the extensional flows experienced during ink jet printing, as it is known that even small fractions of a high molecular weight tails in the molecular weight distribution can have a disproportionate effect on the extensional viscosity and extensional relaxation time measured for a given solution [38].

The influence of polymer concentrations on the zero-shear-rate viscosity of the solutions was investigated using a stress controlled rheometer (Malvern) with a Couette geometry at a constant applied shear rate of $\dot{\gamma} = 30\ \mathrm{s^{-1}}$. The results are presented for each solution in Table 2. As we will demonstrate in the next section from the CaBER-DoS extensional rheology data, the relaxation time of the solutions tested were all below $\lambda < 200$ µs. As a result, the shear rates required to probe shear thinning of the viscosity ($\dot{\gamma} > 5000\ \mathrm{s^{-1}}$) and the oscillatory frequencies required to probe the linear viscoelasticity of the samples ($\omega > 5000$ rad/s) were well beyond the upper limit of our shear rheometer. As a result, no shear thinning data were measured and the shear relaxation time could not be characterized. Trend in the zero-shear-rate viscosity, however, can be observed from Table 2. The shear viscosities of the solutions tested here cover the range of viscosity usually found for industrial inks, $3\ \mathrm{mPa.s} < \eta_0 < 25\ \mathrm{mPa.s}$. The shear viscosity was found to increase with increasing concentration with a power-law exponent that was between 1.5 and 3.0. The CAB-381-2 was found to require least polymer addition to achieve a given solution viscosity while the Paraloid B66 was found to require the most. These effects of concentration appeared to be roughly normalized out if one compared solutions based on reduced concentration instead. The lone exception there was the Vinnol E22/48A which had a markedly higher molecular weight than either of the other two flexible polymer binders, Paraloid B66 and Vinnol E15/45 M. The CAB-381-2 had the highest molecular weight by far, but being a cellulosic polymer, it has a rigid backbone. The impact of polymer rigidity and polymer molecular weight of these binders will be evident in the measurements of extensional rheology.

3. Results and discussions

3.1. CaBER-DoS measurements of Paraloid B66 solutions

Throughout the results and discussion section, we will present CaBER-DoS results for a series of MEK solutions with polymer binders typical of ink jet printing inks. The solutions were developed to explore the effects of solution viscosity, polymer chemistry, polymer backbone rigidity, polymer molecular weight and concentration on extensional rheology and jettability. The trends associated with each of these parameters will be identified and, where possible, better understood through comparison to theory. The results and discussion section will be broken down into two sub-sections. In the first, we will present the experimental measurements and the summary results for the Paraloid B66 solutions in great detail. In the second, we will present the results for the CAB-382-2 and the two Vinnol polymer solutions with a focus on the trends in the data and less on the details of each experiment with an eye towards facilitating comparisons between different polymers and different ink jet fluid compositions.

As described in Section 2, in the CaBER-DoS experiments as well as in many filament thinning or stretching methods, the observed thinning regime is dictated by a balance of the capillary force with the dominant force resisting drainage. The characteristic thinning velocities of the inertio-capillary (U_ρ), visco-capillary (U_η) and elasto-capillary (U_λ) regimes can be calculated from the radius decay for each regime found in Eqs. (1)–(3).

$$U_\rho = 0.48\sqrt{\frac{\sigma}{\rho R}}, \tag{4}$$

$$U_\eta = 0.0709\frac{\sigma}{\eta}, \tag{5}$$

$$U_\lambda = \frac{1}{3}\frac{R}{\lambda_E}. \tag{6}$$

Clasen et al. [23] explained that the lowest characteristic velocity will determine the thinning pathway because the force resisting drainage is largest. A few important observations can be made from Eqs. (4)–(6). Assuming a constant shear viscosity, η, the visco-capillary drainage velocity, U_η , is independent of filament radius. Additionally,

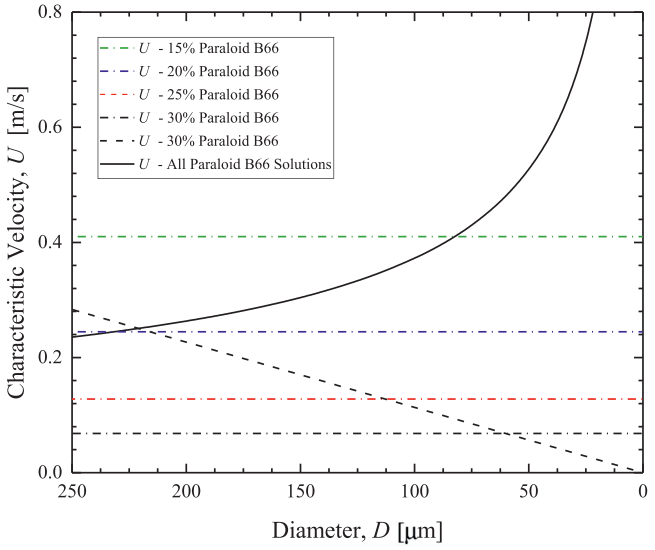

Fig. 2. Characteristic velocities calculated for the filament breakup of various concentrations of Paraloid B-66 into MEK. The solid line represents the evolution of the inertio-capillary velocity, U_ρ, which does not depend on the binder concentration. The dash-dot lines represent the evolutions of the visco-capillary velocities, U_η, for each polymer concentration as shown in the legend. The dashed line respresents the elasto-capillary drainage velocity, U_λ, for the 30wt% Paraloid B-66 solution.

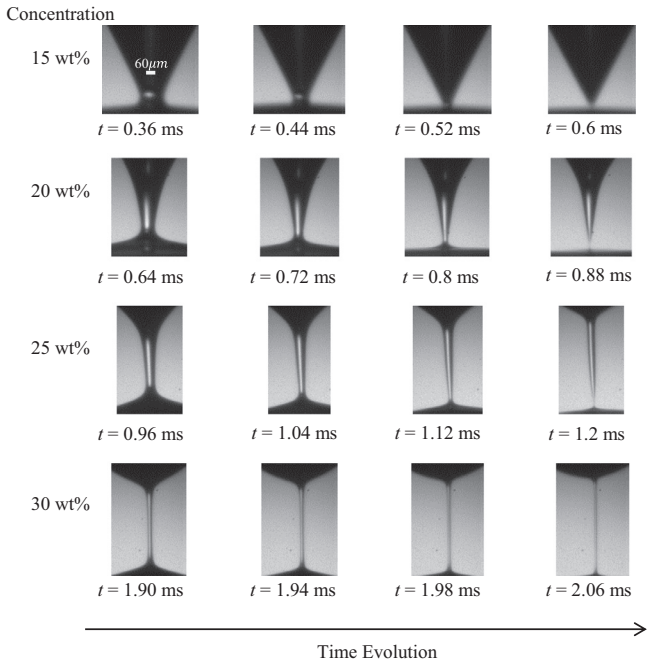

Fig. 3. Evolution of the filament formed in the neck during the breakup of various concentrations of Paraloid B-66 dissolved in MEK during a CaBER-DoS experiments.

inertio-capillary drainage velocity increases as the filament radius decreases while the elasto-capillary drainage velocity decreases. As a result, a series of regime transitions are expected from inertio-capillary to visco-capillary and finally to elasto-capillary if the fluid is viscoelastic. The transition radius from inertio-capillary to visco-capillary drainage can be predicted from the measurements of shear rheology, density and surface tension presented in Tables 1 and 2. This is shown graphically in Fig. 2, where the characteristic velocities for each of the Paraloid B66 solutions is plotted as a function of the filament diameter for diameters below $D < 250$ μm. Note that the evolution of the inertio-capillary drainage velocity is independent of polymer concentration as none of the parameters in Eq. (4) are affected by adding binder. Also note that a line for the elasto-capillary drainage of the 30wt% Paraloid B66 solution has been plotted in Fig. 2. However, this was added for completeness and cannot be added from the shear rheology data because the relaxation time was too small to measure in shear. The CaBER-DoS measurements that follow are necessary in order to calculate the extensional relaxation time, λ_E, needed to feed into Eq. (6). Transitions from inertio-capillary to visco-capillary regimes can be predicted from Fig. 2 for both the 15wt% and the 20wt% Paraloid B66 solutions from the intersection of the lines for U_ρ and U_η. Based on the characteristic velocity calculations, these transitions should occur at diameters of $D = 70$ μm for the 15wt% and $D = 216$ μm for the 20wt% Paraloid B66 solutions. For the highest polymer concentration solutions tested, the transition velocity was expected to be reached at a diameter of $D = 430$ μm and nearly 2 mm for the 25wt% and 30wt% solutions. For each of these systems, the transition was outside of our operation window for the CaBER-DoS measurements and for the case of the 30wt% Paraloid B66 solutions, it was larger than the diameter of the syringe tip used in the experiments. As a result, the 30wt% Paraloid B66 solution was expected to transition from visco-capillary to elasto-capillary drainage without ever experiencing inertio-capillary drainage. These velocity predictions and the transitions that result will be used to determine both extensional viscosity and the extensional relaxation time from the diameter decay measured from the CaBER-DoS experiments. These transitions are also very useful in predicting the lifetime of inelastic fluid filament breaking up into drops during ink-jet printing and seeing exactly how detrimental fluid elasticity can be on the breakup time and distance.

In Fig. 3, a series of images from the time evolution of CaBER-DoS experiments on each of the Paraloid B66 solutions are presented. The images show the necking region between the drop deposited on the substrate and the drop which remains attached to the syringe tip. For a given concentration, these data show the evolution of the neck with time while, for varying concentration, these data show the change in neck shape and breakup regime. All the data are normalized such that time, $t = 0$ ms corresponds to a filament diameter of $D_0 = 250$ μm. The final images are a frame or two ($\sim 10^{-4}$ s) prior to the breakup of the filament. For the lowest concentration shown in Fig. 3, 15wt% Paraloid B66, a triangular conical shape, commonly observed for low viscosity Newtonian fluids is obtained [39]. This focused shape is expected for filaments breaking up in the inertio-capillary regime. This is also the desired breakup shape for continuous ink jet printers because fluids in this regime tend to break up quickly and cleanly with minimal satellite drop generation [40]. As the concentration of the Paraloid B66 was increased, the shape of the necking region was found to change. The cone became progressively less triangular with axial curvature appearing along the neck. This curvature signals the transition to a visco-capillary breakup regime. With higher concentrations, the shear viscosity of the solution was found to increase by a factor of nearly five. This increased viscosity can be observed in the shape of the neck as it becomes extended and narrows. Finally, at a concentration of 30wt% Paraloid B66, the neck can be seen to become highly elongated as it forms a cylindrical filament with little to no axial curvature along the filament. Such long thin filaments are characteristic of elastic fluids and mark the elasto-capillary thinning regime. The first measurable elasto-capillary thinning is observed for the 30wt% Paraloid B66 solution, however, if one looks closely at the final images of the 20wt% and 25wt% Paraloid B66 solutions, the presence of an extremely fine cylindrical filament, hinting at the presence of fluid elasticity, can be observed just prior to breakup. Without a large number of data points to fit to the exponential decay predicted by Eq. (3), it is not possible to make a direct measurement of the relaxation time or the extensional viscosity of the either the 20wt% or 25wt% solution,

however, the recent work of Sur et al. [21] showed that an approximate measure of the relaxation time could be calculated from a single frame of data like that shown in Fig. 3. We will return to the predictions of Sur et al. [21] after fully analysing the extensional rheology of the 30wt% Paraloid B66 solution.

As can be seen from the images in Fig. 3, with increasing polymer concentration, both the breakup length and the breakup time were increased. For the case, case of 20wt% and 25wt% Paraloid B66 solutions, elastic stresses can be neglected, at least until the final 80 μs, and thus the observed increase is due to an increase in the shear viscosity and the resulting increase in the viscous stresses resisting the breakup. For the 30wt% Paraloid B66 solution, the elastic stresses also play a role in resisting the breakup, resulting in an even more significant increase in breakup time and length. To quantify the change, the breakup time increased by 280 μs, 600 μs and 1460 μs as the concentration was increased from 15wt% to 20wt%, 15wt% to 25wt%, and 15wt% to 30wt% respectively. As expected from Eq. (2), the breakup time appeared to grow linearly with shear viscosity for the two inelastic samples. The viscoelastic 30wt% solution showed a marked increase in the breakup time, well beyond what would be predicted by the increased viscosity of the solution only.

In Fig. 4, representational cases of the diameter evolution of the three inelastic Paraloid B66 solutions tested here are presented as a function of time. The uncertainty in the diameter measurements is ±5 μm. A minimum of three independent CaBER-DoS experiments were performed for each solution tested and regression analysis was used to determine the uncertainty of the viscosities and relaxation times calculated from the diameter data. The results shown in Fig. 4 were found to be repeatable to within a few percent in each case. Experimental data are represented in Fig. 4 by symbols, while solid lines representing the inertio-capillary breakup predicted by Eq. (1) and dashed lines representing the visco-capillary breakup predicted by Eq. (2) are superimposed over the experimental data. As predicted by the characteristic velocity maps in Fig. 2, the early stage neck drainage for the 15wt% and the 20wt% Paraloid B66 solutions were found to be inertio-capillary and were well fit by the expected 2/3 power law slope. The transition from the inertio-capillary to the visco-capillary regimes were observed at a diameter of $D = 60$ μm for the 15wt% Paraloid B66 solution and at a diameter of $D = 200$ μm for the 20wt% Paraloid B66 solution. This measurement is in good agreement with the predictions that can be made *a priori* from the characteristic drainage velocities in Eqs. (4) and (5) which are calculated to be $D = 70$ μm and $D = 216$ μm from measurements of the shear viscosity for the 15wt% and 20wt% Paraloid B66 solutions respectively.

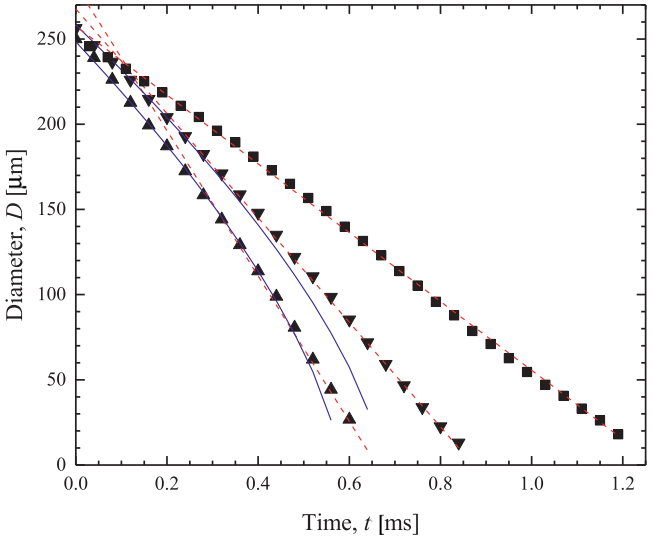

Fig. 4. Diameter evolution of CaBER-DoS experiments on a series of Paraloid B66 solutions in MEK solvent The figure includes experimental data for (▲) 15wt% Paraloid B66, (▼) 20 wt% Paraloid B66 (■) 25 wt% Paraloid B66, along with solid lines (—) representing the fit to the inertio-capillary drainage in Eq. (1) and dashed lines (- -) representing the fit to the visco-capillary drainage in Eq. 2.

Table 3
A comparison of the shear viscosity measured in a Couette rheometer, η_0, to the shear viscosities obtained through a fit of the Eq. (2) to the CaBER-DoS data, η_{fitt}, for a series of Paraloid B66 solutions.

	20wt%	25wt%	30wt%
η_{fit} [mPa.s]	11.0 ± 0.5	18.0 ± 0.7	26.0 ± 0.6
η_0 [mPa.s]	6.9 ± 0.4	13.3 ± 0.7	25.0 ± 1.0

At long times, as the diameter of the neck grew small, a linear diameter decay was observed for both the 15wt% and the 20wt% Paraloid B66 solutions. The 25wt% Paraloid B66 solution showed a linear diameter decay over the entire range of diameters measured as expected from the drainage velocity predictions in Fig. 2. The transition to visco-capillary drainage resulted in a delayed breakup in each case as the filaments would all have failed earlier if the drainage had remained in the inertio-capillary regime. For the 15wt% Paraloid B66 solution, the increase in the breakup time due entirely to viscous effects was only 12 μs, for the 20wt% Paraloid B66 solution, the increase was 130 μs while, for the 25wt% Paraloid B66 solution, the increase is more than 500 μs. By fitting the predictions of Eq. (2) to the data in Fig. 4, the shear viscosity of each solution was calculated. In Table 3, a comparison between the shear viscosity measured in the Couette rheometer and the viscosity obtained from the fit to Eq. (2) is presented. Reasonable agreement between the two viscosities was found, especially for the higher concentration solutions. The fits were found to over predict the shear viscosity measurements from the Couette rheometer at low concentrations. This difference could be the result of the limited number of data points following the inertia-capillary decay that were used to determine the viscosity. The Papageorgiou [28] solution used to fit the data neglects inertia, however, for the two lower concentration samples, the data points used in the fit are close to the transition point from the inertia-capillary to the visco-capillary decay. Thus in this region, inertia could play an important, although secondary, role in the breakup dynamics resulting in the larger values of viscosity seen in low concentration samples. Eggers [41] showed that for a inertia-visco-capillary decay, the prefactor in equation two is reduced from 0.0709 to 0.0304. This change in the prefactor would reconcile the lowest concentration results with the shear viscosity measurements and is likely the more appropriate one to use when so few data points outside of the inertia-capillary regime are used to fit the viscosity.

A representational diameter decay for the 30wt% Paraloid B66 solution is plotted on Fig. 5. This solution is plotted separately from the rest using semi-log axes to emphasize the differences in the diameter decay of the fluid. As with the 25wt% Paraloid B66 solutions, the early diameter decay is linear with time as the drainage is within the visco-capillary regime. However, as the filament approached breakup, a transition to an exponential diameter decay was observed. This observation confirms that the highly elongated, cylindrical filament observed in Fig. 3 was the result of fluid elasticity. From the initial linear diameter decay a fluid viscosity of $\eta_{fit} = 26.0 \pm 0.6$ mPa.s was calculated from Eq. (2) matching the measurements from shear. By fitting the exponential decay prior to breakup to the elasto-capillary decay predicted by Eq. (3), an extensional relaxation time of $\lambda_E = 146 \pm 6$ μs was measured. This value of relaxation time is one of the smallest relaxation times published in the literature, thus demonstrating the versatility and value of the CaBER-DoS technique for measuring the rheology of weakly elastic fluids like printer inks.

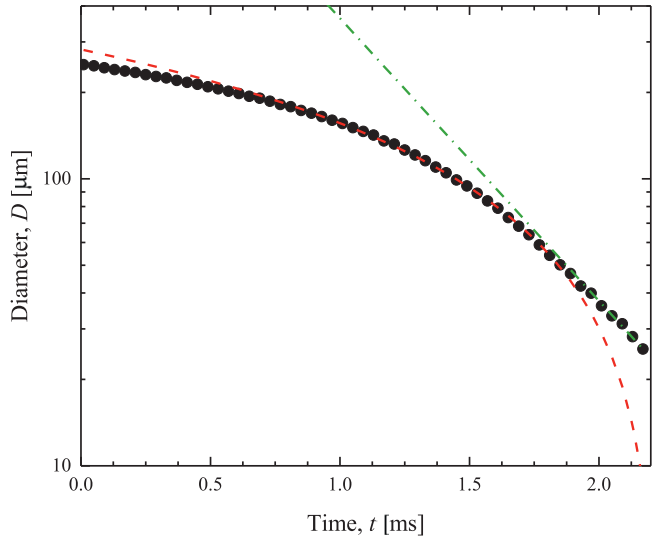

Fig. 5. Diameter decay as a function of time measured using CaBER-DoS for the viscoelastic 30wt% Paraloid B-66 solution in MEK. The data include: the experimental data (•), the fit to the visco-capillary thinning regime in Eq. (2) (– –), and the fit to the elasto-capillary regime given in Eq. (3) (– · –).

Note that, it may be possible to measure the even smaller values of the relaxation time using CaBER-DoS. Sur et al. [21] demonstrated that due to the sharpness in the transition between the inertio-capillary and the elasto-capillary drainage for PEO in a solution of water and glycerol, that relaxation time data could be determined from the diameter measurement of a single image of a viscoelastic filament. In Fig. 3, the presence of a viscoelastic filament is hinted at in the final image of the 25wt% Paraloid B66 solution. In order to calculate the extensional relaxation time, we assume that the filament exists at the transition point between the visco-capillary and the elasto-capillary regimes where $U_\lambda = U_\eta$. Substituting from Eqs. (5) and (6) we find that

$$\lambda_E = 4.7\frac{R\eta}{\sigma}. \tag{7}$$

For the viscoelastic filament captured in Fig. 3, the filament is only one pixel or 5 μm wide. As a result, to form this filament, from Eq. (7), the 20wt% Paraloid B66 solutions can be approximated to have a relaxation time of $\lambda_E = 13.4$ μs.

As described by Sur et al. [21] and by the theoretical predictions of Wagner et al. [42] this value of relaxation time calculated from the final image in Fig. 3 is an underprediction because it assumes that the elastic stresses in the filament are built up instantaneously. In reality, it requires a non-trivial amount of accumulated strain to induce the deformation and elastic stress growth in the polymer chains needed to achieve the constant $Wi = 2/3$ drainage predicted for a viscoelastic CaBER diameter decay. It is interesting to note, that in Sur et al. [21], where the filaments undergo a transition from an inertia-capillary drainage regime to a elasto-capillary drainage regime, the discrepancy between the theoretical predictions and the experimental measurements of the radius at which this transition should occur was off by a factor of five. However, in the experiments presented here, where the transition is from visco-capillary to elasto-capillary, the error between the theoretical calculations in Eq. (7) and the experimental measurements inferred from the 30wt% Paraloid B66 solution data are only approximately 20%. This could be a direct result of the nature of the inertio-capillary and visco-capillary drainage velocities. The visco-capillary drainage velocity is constant, however, as shown by Eq. (4) and observed in Fig. 2, the inertia-capillary drainage velocity increases quickly with decreasing filament radius especially as the radius decreases towards zero. This acceleration of the drainage velocity exacerbates the error between the experimental measurements and the theoretical predictions of the transition radius as it introduces a significant overshoot in the drainage velocity and, as a result, in the extension rate in the filament well beyond the $\dot{\varepsilon} = 2/3\lambda_E$ predicted for CaBER [21]. This is because a finite time is needed for the elastic stress to grow to its steady state value in the thinning filament once the coil stretch transition has been reached beyond a Weissenberg number of $Wi > 1/2$.

We can investigate this transition a little further by plotting the measured extension rate given by

$$\dot{\varepsilon}(t) = -\frac{2}{D(t)}\frac{dD(t)}{dt}, \tag{8}$$

for the 25wt% and the 30wt% Paraloid B66 solutions as a function of time. The results are shown in Fig. 6a. The extension rate measured for the 25wt% Paraloid B66 solution was found to increase monotonically until breakup with extension rates of over $\dot{\varepsilon} > 15,000\,\mathrm{s}^{-1}$ achieved just prior to breakup. The extension rate of the 30wt% Paraloid B66 solution, on the other hand, was found to increase with time, eventually reaching a steady state value of just over $\dot{\varepsilon} = 4100\,\mathrm{s}^{-1}$ after 1.6 ms. Unlike the observations for the transition from inertia-capillary to elasto-capillary drainage [21], no significant overshoot in the extension rate was observed. As a result the, Eq. (7) should be reasonably good for determining the extensional relaxation time from just a single image during the breakup of a viscoelastic fluid filament.

The transient extensional viscosity can also be calculated directly from the diameter decay once the filament has become cylindrical and the flow enters the elasto-capillary regime. The extensional viscosity is given by

$$\eta_E = -\frac{\sigma}{dD(t)/dt}. \tag{9}$$

The extensional viscosity is presented in Fig. 6b alongside the Trouton ratio, $Tr = \eta_E/\eta_0$. Note that in Fig. 6b, the data do not begin until a time of 1.6 ms. Before that time, the filament is not cylindrical and the force balance used to determine the extensional viscosity in Eq. (9) is not valid. The extensional viscosity was found to increase monotonically until filament breakup. Over that time, the extensional viscosity rose from $\eta_E = 0.2$ Pa.s to 0.7 Pa.s or, equivalently, from a Trouton ratio of $Tr = 8$ to $Tr = 29$. Note that for a Newtonian fluid, the Trouton ratio will be exactly $Tr = 3$, so a Trouton ratio of $Tr = 29$ represents a reasonably amount of strain hardening for the 30wt% Paraloid B66 solution. It should be noted that the maximum Trouton ratio varied some from experiment to experiment as it is highly dependent on the final diameter measured at the end of the CaBER-DoS experiment and those diameters are subject to uncertainty that is plus or minus one pixel or ±5 μm. Thus, the extensional viscosity, which requires a derivative of the diameter, tends to amplify the noise in the data, especially as the diameters get towards the resolution limit of the optics. As a result, the data were uniformly cut when the diameters became less than 20 μm to minimize the influence of the measurement uncertainty on the extensional viscosity values presented. The increase of the extensional viscosity just prior to breakup explains the significant breakup delay observed for filaments of Paraloid B66 solutions at the highest polymer concentrations tested. It is interesting to point out that an increase of 5% in polymer concentration can have such a dramatic effect on the breakup time. In this case, increasing the concentration from 25wt% to 30wt% increased the breakup time by nearly 100% and dramatically changed the breakup shape as well. Using CaBER-DoS to gain knowledge of the polymer concentrations where transitions between thinning regimes occur can thus be a crucial tool to aid in the development of fluids for industrial devices such as inkjet printers.

3.2. Comparisons with others industrial binders

In this section, we extend the CaBER-DoS measurements from Paraloid B66 to a series of other polymer binders commonly used in the ink jet printing industry. As described in the section 2.1, all the studied fluids were in the semi-dilute regime. The concentrations that were

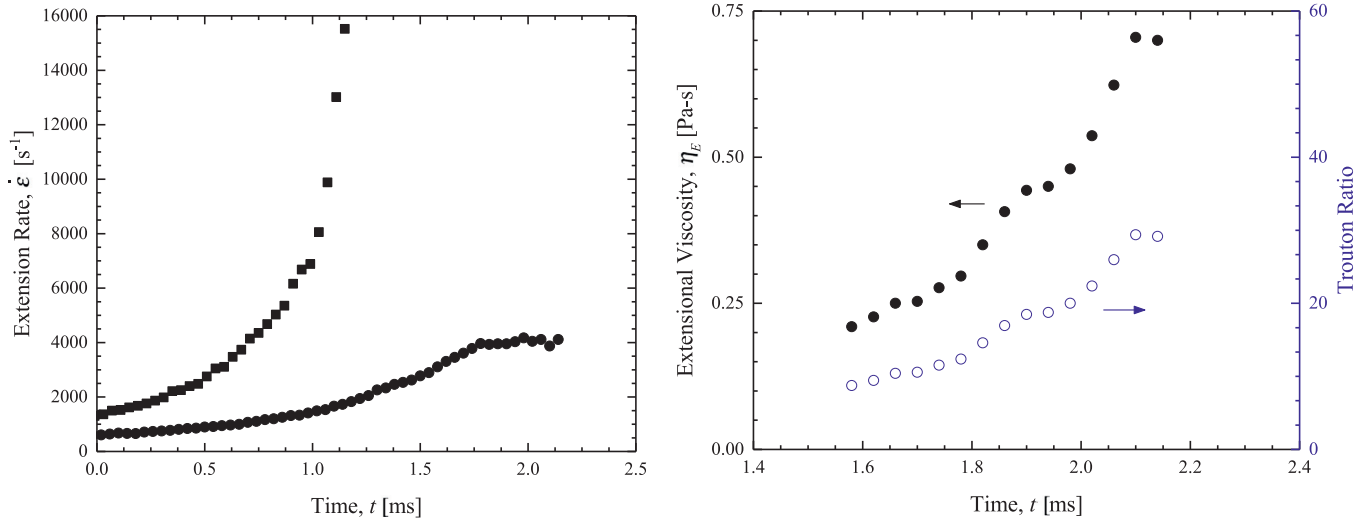

Fig. 6. Results for CaBER-DoS measurements of the 25wt% (■) and 30wt% (•) Paraloid B66 solutions in MEK. In a) the extension rate is plotted as a function of time while in b) the extensional viscosity (•) and Trouton ratio (○) are presented as a function of time.

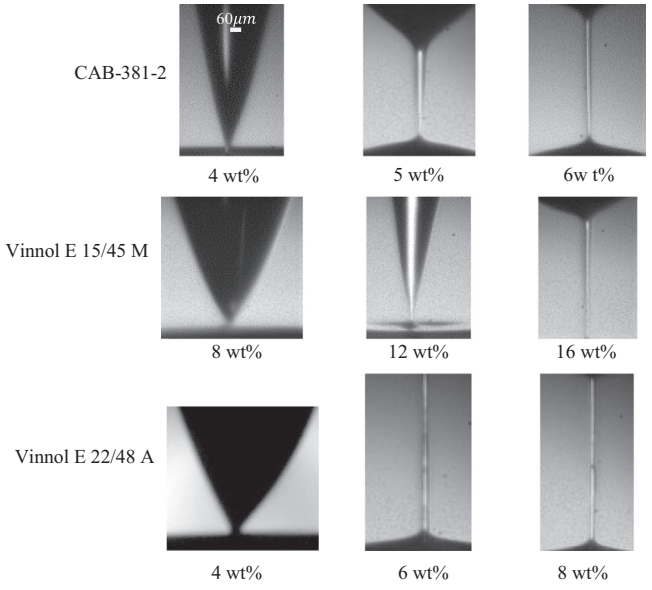

Fig. 7. Breakup shapes obtained for several binders at different concentrations.

used were chosen in order to cover the same range of shear viscosity for each choice of polymer. A description of each polymer, their molecular weight and the shear viscosity at each of the concentrations tested is presented in Tables 1 and 2. Beside their chemical composition, there are a number of other difference between the four binders used of which we should take note. For instance, CAB-381-2 and Vinnol E22/48A each have a significantly higher molecular weight than either Paraloid B66 or Vinnol E15/45 M. For this reason, to achieve similar shear viscosities and reduced concentrations, the solutions of CAB-381-2 and Vinnol E22/48A tested were at lower concentration than either the Paraloid B66 or the Vinnol E15/45 M. Additionally, while the Vinnol and Paraloid polymers are relatively flexible, CAB-381-2 has a rigid backbone that limits its extensibility [43].

The breakup shapes observed during CaBER-DoS measurements of the solutions of CAB-381-2, Vinnol E22/48A and Vinnol E15/45 M in MEK are presented on Fig. 7. At the lowest concentrations tested, all solutions showed a drainage similar to the low concentration results for the Paraloid B66 with a transition from inertia-capillary to visco-capillary breakup. As the concentration of binder was increased, a transitions from visco-capillary to elasto-capillary was observed for all the polymers tested. For the CAB-381-2, this transition occurred between 5wt% and 6wt%. For the, Vinnol E15/45 M, this transition occurred between a concentration of 12wt% and 16wt%. While for the higher molecular weight vinyl polymer, Vinnol E22/48A, this transition occurred at a much lower concentration between 4wt% and 6wt%. Finally, recall that, for the Paraloid B66, this transition was observed between 25wt% and 30wt%. The first observation is that the observed transition to elasto-capillary drainage cannot be directly correlated to the shear viscosity of the solutions. As a specific example, the transition occurs for Paraloid B66 at a concentration with a shear viscosity of 25mPa.s while for the Vinnol E22/48A, the shear viscosity is less than 5mPa.s. Molecular weight clearly plays a role in this transition as increasing the molecular weight from the Vinnol E15/45 M to the Vinnol E22/48A results in a decrease in the transition concentration from 16wt% to 6wt% and a reduction in the shear viscosity of the solution from 17.5 to 6.5mPa.s. Polymer architecture also clearly plays a role in the jettability of a solution. CAB-381-2 has a similarly high molecular weight compared to the Vinnol E22/48A, requires similar concentration, but a much higher viscosity, 16.9mPa.s versus 6.5mPa.s, to transition to an elasto-capillary drainage. This is because the CAB-381-2 is a cellulosic polymer whose backbone is quite rigid. In flow, it behaves like a rigid rod, which can align, but is difficult to deform and stretch. As a results, for the same molecular weight, the extensibility of a rigid polymer is much lower than a flexible polymer leading to a lower relaxation time and a lower extensional viscosity. This can be seen explicitly in relaxation time data presented in Table 4 and the extensional viscosity data shown in Fig. 8.

In Fig. 8, the extension rate, extensional viscosity and Trouton ratio are presented as a function of time for the 6wt% CAB-381-2 solution, the 16wt% Vinnol E15/45 M solution, and the 6wt% Vinnol E22/48A solution in MEK. These three cases were chosen as representative for the CAB and Vinnnol binders as they were the lowest concentration for which an elasto-capillary response was observed. The data for the CAB-381-2 and the lower molecular weight Vinnol E15/45 M solution are quite similar. Each showed an increasing extension rate during the visco-capillary drainage stage before reaching an asymptotic value of just over $\dot{\varepsilon} = 8000\ s^{-1}$ the elasto-capillary drainage just prior to breakup. As shown in Table 4, this extension rate corresponds to a relaxation time of approximately $\lambda_E = 80$ μs. In each case, only the last half dozen or so data points are within the elasto-capillary drainage regime.

From Eq. (9), the extensional viscosity can be calculated from the late time data and is presented in Fig. 8b alongside the Trouton

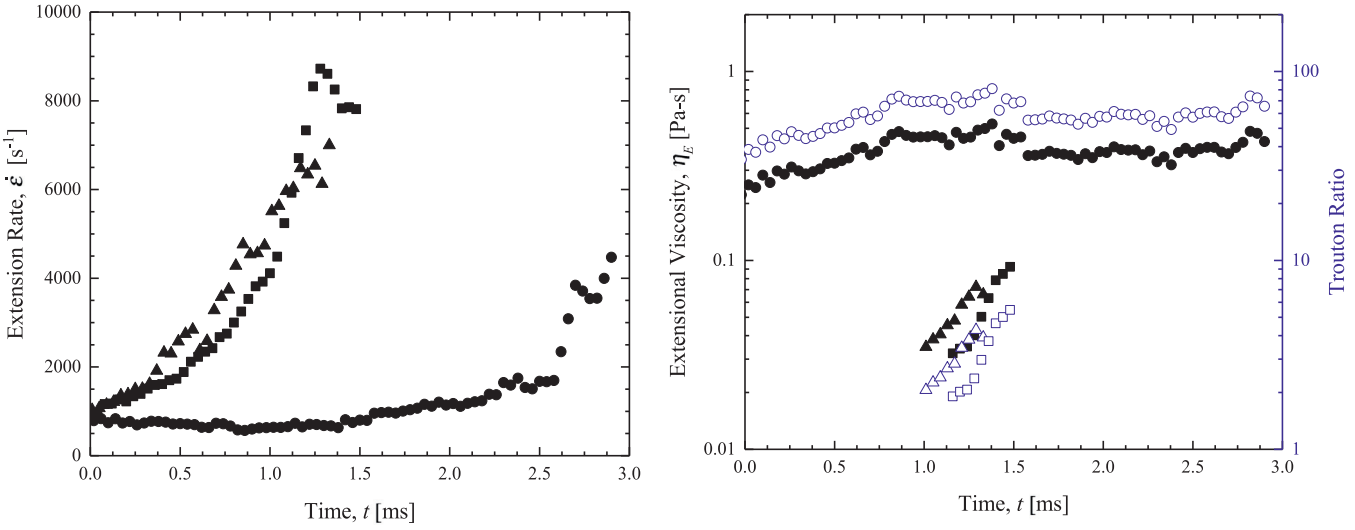

Fig. 8. Results for CaBER-DoS measurements of the 6wt% CAB-381-2 (▲), 16wt% Vinnol E15/45 M (■), and 6wt% Vinnol E22/48A (•) solutions in MEK. In a) the extension rate is plotted as a function of time while in b) the extensional viscosity and Trouton ratio are presented as solid and hollow symbols respectively as a function of time.

Table 4
Rheological data for the solutions of the four different polymer binders studied. Data include the shear viscosity measured in a Couette rheometer, η_0, the shear viscosities, η_{fit}, obtained through a fit of the Eq. (2) to the CaBER-DoS data, and the extensional relaxation time, λ_E, obtained through a fit to Eq. (3) to the CaBER-DoS data.

Concentration [wt%]	η_0 [mPa.s]	η_{fit} [mPa.s]	λ_E [μs]
	CAB-381-2		
5	9.4 ± 0.5	12 ± 0.4	–
6	16.9 ± 0.9	17 ± 0.2	71 ± 6
	Vinnol E15/45M		
12	7.9 ± 0.4	11 ± 0.5	–
16	17.5 ± 0.9	18 ± 0.5	78 ± 6
	Vinnol E22/48A		
6	6.0 ± 0.3	–	740 ± 40
8	8.1 ± 0.4	–	1000 ± 50
10	13.0 ± 0.7	–	1700 ± 70
	Paraloid B66		
20	6.9 ± 0.4	11 ± 0.4	–
25	13.3 ± 0.7	18 ± 0.6	–
30	25.0 ± 1.0	26 ± 0.5	146 ± 6

ratio. For both the the CAB-381-2 and the lower molecular weight Vinnol E15/45 M solutions, little strain hardening is observed with Trouton ratios of $Tr = 4$ or 5 achieved before filament breakup. This is a reflection of the low molecular weight of the Vinnol E15/45 M and the rigidity of the CAB-381-2 [43]. By contrast, the high molecular weight Vinnol E22/48A transitions to the elasto-capillary drainage regime at a much lower extension rate, $\dot{\varepsilon} = 850\,\mathrm{s}^{-1}$, resulting in measured extensional relaxation time of $\lambda_E = 740$ μs. At long times and diameters below about $D < 100$ μm, the exponential decay in the diameter decay data transitioned back to a linear decay with time resulting in an upturn in the extension rate data beyond $t = 1.5$ s. This occurred because the finite extensibility of the 6% Vinnol E22/48A solution was reached at a steady-state extensional viscosity of $\eta_E = 0.5$mPa.s and a Trouton ratio of $Tr = 70$. In this regime, the polymer solution again behaves like an inelastic fluid with a constant, albeit with a much larger viscosity. Similar results were observed for the 8wt% and 10wt% Vinnol E22/48A solutions tested. A summary of these data can be found in Table 4.

For the case of Vinnol E22/48A, enough experiments were performed at concentrations within the elasto-capillary regime that an approximate scaling could be calculated for the relaxation time with reduced concentration, c/c^*. For Vinnol E22/48A, the relaxation time was found to increase as $\lambda_E \propto (c/c^*)^{1.6}$. For a dilute solution, $c/c^* < 1$, the relaxation time has been found experimentally to increase like $\lambda_E \propto (c/c^*)^{0.65}$ [9,21]. For semi-dilute polymer solutions like the Vinnol E22/48A studied here, the extensional relaxation time was found to increase with reduced concentration as, $\lambda_E \propto c/c^*$ when the reduced concentration was just above one, $c/c^* \sim 1$, [44] and with a slightly stronger power-law dependence, $\lambda_E \propto (c/c^*)^{4/3}$, when the reduced concentrations significantly larger than one, $c/c^* > 1$ [45]. This stronger power-law dependence for systems like the Vinnol E22/48A studied here, was argued to be the result of the presence of entanglements and shear thinning and solvent quality [44].

As seen from Eq. (7), it is the extensional relaxation time along with the shear viscosity of a given fluid that will dictate whether the elasto-capillary flow regime will be observable in CaBER-DoS or during the breakup of a jet into drops during inkjet print. Rearranging Eq. (7), we find for the elasto-capillary drainage regime to be visible, $\lambda_E/\eta > 4.7 R_{\min}/\sigma$. For the case or the solutions studied here with MEK as the solvent and a 5 μm resolution of our optics, the ratio of relaxation time to shear viscosity must be larger than $\lambda_E/\eta > 9.8\mathrm{x}10^{-4}\mathrm{Pa}^{-1}$ in order for an viscoelastic filament to be observed. In reality, however, for the elasticity of the fluid to have a significant impact on the drainage and the time to breakup, elastic effects should become important at a radius much larger than the optical resolution of the high-speed video camera. In Fig. 9, the time required for each solution to break up from an initial diameter of $D = 250$ μm is plotted as a function of the zero-shear-rate viscosity of each fluid. An approximately linear increase with increasing shear viscosity is observed for all the inelastic solutions. The onset of elasto-capillary drainage breaks down this linear relationship. This is easiest to observe in Fig. 8 for the case of the higher molecular weight Vinnol E22/48A because of its large relaxation time and Trouton ratio. Note, that even though they are not easy to observe in Fig. 8, small deviations from linearity do exist for the highest concentrations of the Paraloid-B66, CAB-381-2 and Vinnol E15/45 M tested. They are difficult to see because of the extremely short relaxation times of these solutions and because the magnitude of the deviation found for the Vinnol E22/48A required the x-axis to be stretched to accommodate the data.

The variation of the data with shear viscosity for a Newtonian fluid can be understood by manipulating Eqs. (1), (2), (4) and (5) to find the breakup time for a fluid initially in the inertio-capillary drainage

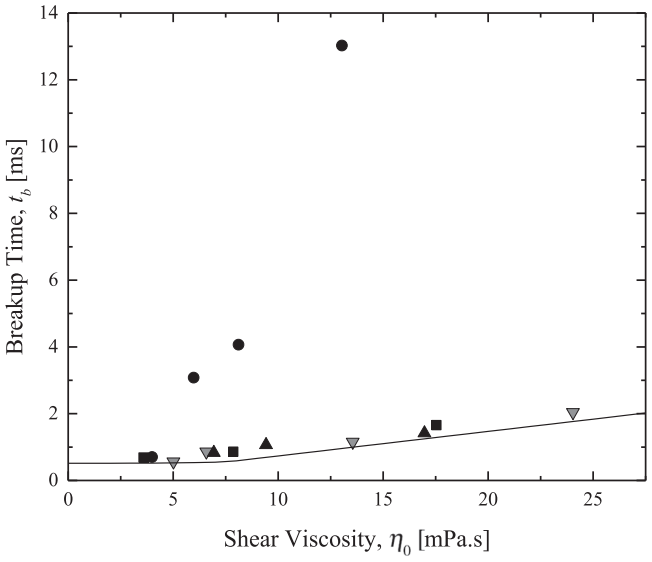

Fig. 9. Breakup time from $D = 250$ μm for each of the solutions tested in CaBER-DoS as a function of shear viscosity of each solution. The data include: CAB-381-2 (▲), Vinnol E15/45 M (■), Vinnol E22/48A (•) and Paraloid B66 (▼) solutions in MEK. A line showing the theoretical prediction of breakup time for a Newtonian fluid given by Eq. (10) is superimposed over the data.

regime and transitioning to the visco-capillary regime when $U_\rho = U_\eta$. The breakup time becomes

$$t_b = \left(\frac{\rho}{0.26\,\sigma}\right)^{1/2}\left(R_0^{3/2} - R_{trans}^{3/2}\right) + \frac{R_{trans}}{0.0709}\,\frac{\eta}{\sigma}, \tag{10}$$

where the R_{trans} is the radius at which the drainage transitions from the inertia-capillary to the visco-capillary regime

$$R_{trans} = 45.8\,\frac{\eta^2}{\rho\,\sigma}. \tag{11}$$

The theoretical predictions of Eq. (10) do a good job of predicting the breakup time and its change with increasing solution viscosity. Note that the breakup time does not quite increase linearly with shear viscosity as the transition radius depends on the viscosity of the solutions. As a result, increasing viscosity increases the transition radius and causes the filament decay to reside within the slower visco-capillary regime for more time. Beyond a viscosity of $\eta_0 > 25$mPa.s, the drainage from $D = 250$ μm is entirely within the visco-capillary regime. A similar approach can be attempted for a transition from a visco-capillary to an elasto-capillary drainage, but here one has two fluid properties that are varying; viscosity and relaxation time. As a result, a universal line like the one from Eq. (10) cannot be superimposed on the data in Fig. 9. Nonetheless, the breakup time for the viscoelastic solutions studied here can be calculated from theory once the relaxation time has been fit. This of course is a bit of a recursive argument as it is this same theory that we are using to fit the relaxation time in the first place. Here the visco-capillary breakup time becomes

$$t_{b,vc} = \frac{R_0 - R_{trans,vc}}{0.0709}\,\frac{\eta}{\sigma} - 3\lambda_E \ln\left(\frac{R_{cut-off}}{R_{trans,vc}^{4/3}}\left(\frac{2\sigma}{G}\right)^{1/3}\right) \tag{12}$$

As in Eq. (7), the transition radius is given by $R_{trans,vc} = \frac{\lambda_E \sigma}{4.7\eta}$ and $R_{cut\text{-}off} = 5$ μm is the cut-off radius where we assume the filament has broken. Here we chose the resolution of our optics for the cut-off radius. This analysis assumes the polymer does not reach its finite extensibility limit during the necking of the fluid filament. As a result, this approach does not work well for the high molecular weight Vinnol E22/48A solutions, as it over predicting the breakup by quite a significant amount. Unfortunately, to understand the breakup dynamics of these highly elastic systems a full FENE-P solution like that found in Wagner et al. [42] is likely necessary. Of course this is only possible after fully characterizing the rheology of the fluid like we have done in this paper.

4. Conclusions

In this paper, the capillary thinning dynamics of a series of solutions containing polymers commonly used in the coating industry as low-viscosity printing inks were studied. Four different polymer binders were studied in the same MEK solvent. These polymers included one acrylic polymer (Paraloid B66), one cellulose polymer (CAB-381-2) and two vinyl polymers of a low (Vinnol E15/45 M) and higher (Vinnol E22/48A) molecular weight. The dripping-onto-substrate capillary breakup extensional rheometry (CaBER-DoS) method was used to characterize the extensional rheology for solutions with viscosities as low as $\eta_0 = 3.5$mPa.s and relaxation times ranging from unmeasurable all the way to $\lambda_E = 1700$ μs. This technique is based on the measurement of the decay of a fluid filament under the influence of surface tension and has been shown to be capable of measuring extremely small relaxation times for weakly elastic liquids. Here we showed that by utilizing a single image in time, relaxation times as low as $\lambda_E = 13.4$ μs could be measured from the diameter decay of these model inkjet fluids. These relaxation times are the smallest ever reported in the literature.

The influence of the polymer concentration on the dynamics of filament breakup was investigated for each polymer solution and the results were compared to those obtained with different polymer binders. With an increase in polymer concentration, a critical concentration was identified for the transition between the inertio-capillary, the visco-capillary and the elasto-capillary breakup regimes. These values were found to vary quite strongly with the polymer molecular weight as well as with its backbone chemistry and its resulting rigidity. Increasing molecular weight and decreasing backbone rigidity were both found to reduce the concentrations needed to observe elasto-capillary drainage while increasing the relaxation time and extensional viscosity of the resulting solutions. Within the elasto-capillary breakup regime, the transient extensional viscosity resulted in Trouton ratios ranging from just above the Newtonian limit of $Tr = 3$ to values close to $Tr = 100$.

With the onset of elasto-capillary breakup at moderate to high polymer concentrations, a delay in the filament breakup was observed due to the rise of viscous and elastic stresses. The change in breakup time was predicted by a series of simple theoretical models. These viscous and viscoelastic breakup time delays, if significant, could be detrimental to most ink jet printing applications. The CaBER-DoS technique, thus appears to be an extremely useful technique for evaluating potential fluids for their jettability and suitability for use in ink jet applications.

Acknowledgment

The authors would like to thank the Markem-Imaje Corporation for funding this research and Christian Clasen of KU Leuven for use of the Edgehog software.

References

[1] B.-J. de Gans, P.C. Duineveld, U.S. Schubert, Inkjet printing of polymers: state of the art and future developments, Adv. Mater 16 (2004) 203–213.
[2] O.A. Basaran, H. Gao, P.P. Bhat, Nonstandard inkjets, Annu. Rev. Fluid Mech. 45 (2013) 85–113.
[3] G.D. Martin, S.D. Hoath, I.M. Hutchings, Inkjet printing - the physics of manipulating liquid jets and drops, J. Phys. 105 (2008) 012001.
[4] N.F. Morrison, O.G. Harlen, Viscoelasticity in inkjet printing, Rheol. Acta 49 (2010) 619–632.
[5] S.D. Hoath, D.C. Vadillo, O.G. Harlen, C. McIlroy, N.F. Morrison, W.-K. Hsiao, T.R. Tuladhar, S. Jung, G.D. Martin, I.M. Hutchings, Inkjet printing of weakly elastic polymer solutions, J. Non-Newt. Fluid Mech 205 (2014) 1–10.
[6] Y. Christanti, L.M. Walker, Surface tension driven jet break up of strain-hardening polymer solutions, J. Non-Newt. Fluid Mech. 100 (2001) 9–26.
[7] Y. Christanti, L.M. Walker, Effect of fluid relaxation time of dilute polymer solutions on jet breakup due to a forced disturbance, J. Rheol. 46 (2002) 733–748.
[8] M. Gordon, J. Yerushalmi, R. Shinnar, Instability of jets of Non-Newtonian fluids, J. Rheol. 17 (1973) 303–324.

[9] J. Dinic, Y. Zhang, L.N. Jimenez, V. Sharma, Extensional relaxation times of dilute, aqueous polymer solutions, ACS Macro Lett 4 (2015) 804–808.
[10] J. Dinic, L.N. Jimenez, V. Sharma, Pinch-off dynamics and dripping-onto-substrate (DoS) rheometry of complex fluids, Lab Chip 17 (2017) 460–473.
[11] G.H. McKinley, T. Sridhar, Filament stretching rheometry, Annu. Rev. Fluid Mech. 34 (2002) 375–415.
[12] S.H. Spiegelberg, G.H. McKinley, Stress relaxation and elastic decohesion of viscoelastic polymer solutions in extensional flow, J. Non-Newt. Fluid Mech. 67 (1996) 49–76.
[13] A.V. Bazilevsky, V.M. Entov, A.N. Rozhkov, Liquid filament microrheometer and some of its applications, in: D.R. Oliver (Ed.), Proc. Third European Rheology Conference, Edinburgh, 1990, pp. 41–43.
[14] S.L. Anna, G.H. McKinley, Elasto-capillary thinning and breakup of model elastic liquids, J. Rheol. 45 (2001) 115–138.
[15] D.C. Vadillo, W. Mathues, C. Clasen, Microsecond relaxation processes in shear and extensional flows of weakly elastic polymer solutions, Rheologica Acta 51 (2012) 755–769.
[16] D.C. Vadillo, T.R. Tuladhar, A.C. Mulji, S. Jung, S.D. Hoath, M.R. Mackley, Evaluation of the inkjet fluid's performance using the "Cambridge Trimaster" filament stretch and break-up device, J. Rheol. 54 (2010) 261–282.
[17] L. Campo-Deano, C. Clasen, The slow retraction method (SRM) for the determination of ultra-short relaxation times in capillary breakup extensional rheometry experiments, J. Non-Newt. Fluid Mech. 165 (2010) 1688–1699.
[18] B. Keshavarz, V. Sharma, E.C. Houze, M.R. Koerner, J.R. Moore, P.M. Cotts, P. Threlfall-Holmes, G.H. McKinley, Studying the effects of elongational properties on atomization of weakly viscoelastic solutions using Rayleigh Ohnesorge Jetting Extensional Rheometry (ROJER), J. Non-Newt. Fluid Mech. 222 (2015) 234–247.
[19] L. Rayleigh, On the instability of jets, Proc. Lond. Math. Soc. 10 (1879) 4–13.
[20] E. Greiciunas, J. Wong, I. Gorbatenko, J. Hall, M.C.T. Wilson, N. Kapur, O.G. Harlen, D. Vadillo, P. Threlfall-Holmes, Design and operation of a Rayleigh Ohnesorge jetting extensional rheometer (ROJER) to study extensional properties of low viscosity polymer solutions, J. Rheol. 61 (2017) 467–476.
[21] S. Sur, J.P. Rothstein, Drop breakup dynamics of dilute polymer solutions: effect of molecular weight, concentration and viscosity, J. Rheol. 62 (2018) 1245–1259.
[22] C. Clasen, Capillary breakup extensional rheometry of semi-dilute polymer solutions, Korea-Australia Rheol. J. 22 (2010) 331–338.
[23] C. Clasen, P.M. Phillips, L. Palangetic, J. Vermant, Dispensing of Rheologically complex fluids: the map of misery, AIChE J 58 (2012) 3242–3255.
[24] G.H. McKinley, Visco-elasto-capillary thinning and break-up of complex fluids, in: D.M. Binding, K. Walters (Eds.), Annual Rheology Reviews, The British Society of Rheology, Aberystwyth, Wales, UK, 2005, pp. 1–49.
[25] C. Clasen, P.M. Phillips, L. Palangetic, Dispensing of rheologically complex fluids: the map of misery, AIChE J. 58 (2012) 3242–3255.
[26] G.H. McKinley, Visco-elasto-capillary thinning and breakup of complex fluids, in: D.M. Binding, K. Walters (Eds.), Annual Rheology Reviews, British Society of Rheology, Aberystwyth, 2005, pp. 1–48.
[27] J. Dinic, Y. Zhang, L.N. Jimenez, V. Sharma, Extensional relaxation times of dilute, aqueous polymer solutions, ACS Macro Lett. 4 (2015) 804–808.
[28] D.T. Papageorgiou, On the breakup of viscous liquid threads, Phys. Fluids 7 (1995) 1529–1544.
[29] V.M. Entov, E.J. Hinch, Effect of a spectrum of relaxation times on the capillary thinning of a filament of elastic liquid, J. Non-Newt. Fluid Mech. 72 (1997) 31–53.
[30] C. Clasen, J. Eggers, M.A. Fontelos, J. Li, G.H. McKinley, The beads-on-string structure of viscoelastic threads, J. Fluid Mech. 556 (2006) 283–308.
[31] C. Clasen, J.P. Plog, W.M. Kulicke, M. Owens, C.W. Macosko, L.E. Scriven, M. Verani, G.H. McKinley, How dilute are dilute solutions in extensional flows? J. Rheol. 50 (2006) 849–881.
[32] J. Brandrup, E.H. Immergut, Polymer Handbook, John Wiley & Sons, New York, 1989.
[33] R. Crooks, J.J. Cooper-White, D.V. Boger, The role of dynamic surface tension and elasticity on the dynamics of drop impact, Chem. Eng. Sci. 56 (2001) 5575–5592.
[34] J.P. Rothstein, Transient extensional rheology of wormlike micelle solutions, J. Rheol. 47 (2003) 1227–1247.
[35] M. Doi, S.F. Edwards, The Theory of Polymer Dynamics, Oxford University Press, Oxford, 1986.
[36] P.K. Bhattacharjee, J. Oberhauser, G.H. McKinley, L.G. Leal, T. Sridhar, Extensional rheometry of entangled solutions, Macromol 35 (2002) 10131–10148.
[37] J.P. Rothstein, G.H. McKinley, A comparison of the stress and birefringence growth of dilute, semi-dilute and concentrated polymer solutions in uniaxial extensional flows, J. Non-Newt. Fluid Mech. 108 (2002) 275–290.
[38] L. Palangetic, N.K. Reddy, S. Srinivasan, R.E. Cohen, G.H. McKinley, C. Clasen, Dispersity and spinnability: why highly polydisperse polymer solutions are desirable for electrospinning, Polymer 55 (2014) 4920–4931.
[39] L. Campo-Deano, C. Clasen, The slow retraction method (SRM) for the determination of ultra-short relaxation times in capillary breakup extensional rheometry experiments, J. Non-Newt. Fluid Mech. (2010) 2010.
[40] M. Rosello, G. Maîtrejean, D.C.D. Roux, P. Jay, B. Barbet, J. Xing, Influence of the Nozzle Shape on the Breakup Behavior of Continuous Ink Jets, J. Fluid Eng. 140 (2018) 031202.
[41] J. Eggers, Nonlinear dynamics and breakup of free-surface flows, Rev. Mod. Phy. 69 (1997) 865–929.
[42] C. Wagner, L. Bourouiba, G.H. McKinley, An analytic solution for capillary thinning and breakup of FENE-P fluids, J. Non-Newt. Fluid Mech 218 (2015) 53–61.
[43] S.L. Ng, R.P. Mun, D.V. Boger, D.F. James, Extensional viscosity measurements of dilute solutions of various polymers, J. Non-Newt. Fluid Mech 65 (1996) 291–298.
[44] J. Dinic, M. Biagioli, V. Sharma, Pinch-off dynamics and extensional relaxation times of intrinsically semi-dilute polymer solutions characterized by dripping-onto-substrate rheometry, J. Poly. Sci. Part B: Poly. Phys. 55 (2017) 1692–1704.
[45] O. Arnolds, H. Buggisch, D. Sachsenheimer, N. Willenbacher, Capillary breakup extensional rheometry (CaBER) on semi-dilute and concentrated polyethyleneoxide (PEO) solutions, Rheologica acta 49 (2010) 1207–1217.